© 2014 by The American Society for Biochemistry and Molecular Biology, Inc.
This paper is available on line at http://www.mcponline.org

Regulation Dynamics of *Leishmania* Differentiation: Deconvoluting Signals and Identifying Phosphorylation Trends*[S]

Polina Tsigankov‡, Pier Federico Gherardini§, Manuela Helmer-Citterich§, Gerald F. Späth¶, Peter J. Myler‖‡‡, and Dan Zilberstein‡§§**

Leishmania **are obligatory intracellular parasitic protozoa that cause a wide range of diseases in humans, cycling between extracellular promastigotes in the mid-gut of sand flies and intracellular amastigotes in the phagolysosomes of mammalian macrophages. Although many of the molecular mechanisms of development inside macrophages remain a mystery, the development of a host-free system that simulates phagolysosome conditions (37 °C and pH 5.5) has provided new insights into these processes. The time course of promastigote-to-amastigote differentiation can be divided into four morphologically distinct phases: I, signal perception (0–5 h after exposure); II, movement cessation and aggregation (5–10 h); III, amastigote morphogenesis (10–24 h); and IV, maturation (24–120 h). Transcriptomic and proteomic analyses have indicated that differentiation is a coordinated process that results in adaptation to life inside phagolysosomes. Recent phosphoproteomic analysis revealed extensive differences in phosphorylation between promastigotes and amastigotes and identified stage-specific phosphorylation motifs. We hypothesized that the differentiation signal activates a phosphorylation pathway that initiates** ***Leishmania*** **transformation, and here we used isobaric tags for relative and absolute quantitation to interrogate the dynamics of changes in the phosphorylation profile during** ***Leishmania donovani*** **promastigote-to-amastigote differentiation. Analysis of 163 phosphopeptides (from 106 proteins) revealed six distinct kinetic profiles; with increases in phosphorylation predominated during phases I and III, whereas phases II and IV were characterized by greater dephosphorylation. Several proteins (including a protein kinase) were phosphorylated in phase I after exposure to the complete differentiation signal (*** ***i.e.*** **signal-specific; 37 °C and pH 5.5), but not after either of the physical parameters separately. Several other protein kinases (including regulatory subunits) and phosphatases also showed changes in phosphorylation during differentiation. This work constitutes the first genome-scale interrogation of phosphorylation dynamics in a parasitic protozoa, revealing the outline of a signaling pathway during** ***Leishmania*** **differentiation.**

The mass spectrometry proteomics data have been deposited to the ProteomeXchange Consortium (identifier PXD000671). Data can be viewed using ProteinPilot™ software. ***Molecular & Cellular Proteomics 13: 10.1074/mcp.M114.037705, 1787–1799, 2014.***

Protozoan parasites of the genus *Leishmania* are the causative agents of leishmaniasis in humans, which can manifest as hepatosplenomegaly, ulcerative skin lesions, or destructive mucosal inflammation and damage to the mucosal tissues (1, 2). The parasites cycle between two major forms in two distinct environments, starting out as flagellated extracellular promastigotes in the alimentary tract of the female sand fly and subsequently differentiating into immotile intracellular amastigotes within the phagolysosomes of mammalian macrophages (1). While cycling between these two forms, parasites encounter two distinct environments to which they must quickly adapt. As extracellular promastigotes, parasites are surrounded by the sugar-rich, slightly alkaline environment of the fly's mid-gut, which has a mean temperature of 26 °C. Intracellular amastigotes encounter the sugar-poor, fatty-acid- and amino-acid-rich acidic environment of the phagolysosome at the elevated temperatures of the skin and viscera (3, 4). To enable molecular insight into *Leishmania* development, an axenic host-free system that simulates *Leishmania* differentiation by exposing promastigotes to a lysosome-like environment was developed (5–7). These studies indicated that concomitant exposure to acidic pH levels (usually pH 5.5) and high temperatures (33 °C and 37 °C for cutaneous and visceral strains, respectively) provides the sig-

From the ‡Faculty of Biology, Technion-Israel Institute of Technology, Haifa 32000, Israel; §Center for Molecular Bioinformatics, Department of Biology, University of Rome Tor Vergata, Rome, Italy; ¶Institut Pasteur, CNRS URA2581, Unité de Parasitologie moléculaire et Signalisation, 75015 Paris, France; ‖Seattle Biomedical Research Institute, Seattle, Washington 98109; **Department of Global Health, University of Washington, Seattle, Washington 98195; ‡‡Department of Biomedical Informatics and Medical Education, University of Washington, Seattle, Washington 98195

Received January 16, 2014, and in revised form, April 13, 2014
Published, MCP Papers in Press, April 16, 2014, DOI 10.1074/mcp.M114.037705
Author contributions: G.F.S. and D.Z. designed research; P.T. performed research; P.T., P.G., M.H., and P.J.M. analyzed data; P.T., P.J.M., and D.Z. wrote the paper.

ASBMB MOLECULAR & CELLULAR PROTEOMICS MCP

nals that lead promastigotes to start differentiation into amastigotes, a process that is completed within 5 days (8).

Time-course analyses carried out in *Leishmania donovani* indicated that differentiation is a highly regulated and coordinated process. Based on cell morphology, Barak *et al.* divided differentiation into four phases: phase I (the first 5 h after exposure of promastigotes to the differentiation signal), which is dedicated to signal perception; phase II (5–10 h after signal exposure), during which the parasites cease movement and start to aggregate; phase III (10–24 h), when cells undergo morphological change into amastigote-shaped cells; and phase IV (24–120 h), during which the amastigotes undergo maturation (8). Significant changes in mRNA (9, 10) and protein abundance (11), as well as in the rate of translation (12), allow the parasites to adjust to an amastigote lifestyle by re-tooling their energy metabolism from glycolysis to fatty-acid- and amino-acid-based catabolism. For example, the transition is accompanied by an increase in protein abundance and activity rates of gluconeogenic enzymes, as it becomes an essential pathway in amastigotes (11, 13, 14). These biochemical changes are initiated in the middle of the third phase of differentiation, while parasites undergo morphogenesis (15), and appear mostly regulated by changes in translation rate and/or post-translational processing (10). Indeed, post-translational modifications occur at all phases of promastigote-to-amastigote differentiation. These include protein glycosylation, methylation, acetylation, and phosphorylation (16). In contrast, most changes in protein abundance at the beginning of differentiation are regulated by mRNA, and there are a number of transient changes in mRNA and protein abundance (10).

In yeast, protein phosphorylation is estimated to affect 30% of the proteome and is a major regulatory mechanism that controls many basic cellular processes (17). Although the *Leishmania* phosphoproteome has not yet been analyzed to completion, it is reasonable to assume that a similar portion of the proteome is phosphorylated. Interestingly, the majority of phosphoproteins identified to date are differentially regulated between promastigotes and amastigotes, with more phosphorylation in the latter (18–21). This supports the notion that protein phosphorylation plays an important role during *Leishmania* differentiation and is likely controlled by stage-regulated protein kinases and phosphatases.

It is likely that a complex network of phosphorylation and dephosphorylation events constitutes a regulatory pathway controlling *Leishmania* differentiation. To evaluate protein phosphorylation during differentiation and, in particular, to identify early phosphorylation events that might be part of the signaling pathway that initiates differentiation, we employed quantitative proteomics (iTRAQ[1]) to determine protein phosphorylation dynamics during axenic *L. donovani* promastigote-to-amastigote differentiation. These analyses revealed a number of changes in protein phosphorylation as early as phase I, several of which occurred only when promastigotes were exposed to the complete differentiation signal (*i.e.* 37 °C and pH 5.5). This work constitutes the first time-course analysis of the quantitative phosphorylation of *Leishmania* promastigote-to-amastigote differentiation and identifies the protein kinase pathway that may initiate this process in *L. donovani*.

[1] The abbreviation used is: iTRAQ, isobaric tags for relative and absolute quantitation.

EXPERIMENTAL PROCEDURES

L. donovani Cell Culture—A cloned line of *L. donovani* 1SR was used in all experiments. Promastigotes and amastigotes were grown as described (8). Promastigote-to-amastigote differentiation in axenic culture was carried out as described by Barak *et al.* (8). Briefly, late-log promastigotes were transferred from promastigote medium at 26 °C and pH 7.4 to amastigote medium at 37 °C, pH 5.5, and 5% CO_2. Twenty-four hours after the initiation of differentiation, cells were split 1:10 in prewarmed amastigote medium.

Protein Extraction and Phosphopeptide Enrichment—Mid-logarithmic phase promastigotes (1×10^7 to 1.5×10^7 cells/ml) were washed three times in ice-cold phosphate-buffered saline (PBS) and snap frozen in liquid nitrogen. Differentiating *Leishmania* at different time points in differentiation and amastigote cell cultures (1×10^7 to 1.5×10^7 cells/ml) were washed three times in ice-cold Earle's buffer at pH 5.5 and snap frozen in liquid nitrogen. For the signal-specific phosphoproteomic experiment, the culture that was exposed to the full signal (*i.e.* temperature and pH) and the culture that was exposed to pH 5.5 were washed with ice-cold Earle's buffer at pH 5.5, and the culture that was exposed to 37 °C was washed with ice-cold PBS. Both buffers that were used for washes were supplemented with phosphatase inhibitors (5 mM NaF, 5 mM sodium orthovanadate, and 10 mM β-glycerophosphate). Frozen cell pellets were lysed and proteins were extracted as in Ref. 18. Proteins were trypsinized and phosphopeptide enrichment was conducted as in Ref. 18. The eluant was frozen at −80 °C and lyophilized to dryness.

Relative and Absolute Quantitation (iTRAQ) Tag Labeling—Peptides were resuspended with 0.5 M triethylammonium bicarbonate (TAEB) (pH 8.5). A unique iTRAQ label (4-plex) was added to each sample. Samples were vortexed and centrifuged. The labeling reaction was conducted for 60 min at room temperature (23 °C). Four separately labeled samples were pooled and vacuum concentrated to remove the organic solvent component prior to LC-MS/MS analysis.

LC-MS/MS Analysis—iTRAQ-labeled peptides were combined and separated via strong cation exchange HPLC. Strong cation exchange fractions containing peptides were then reduced in volume by a SpeedVac and analyzed via LC-MS/MS. The length of the reverse gradient used was adjusted from 1 to 2 h for fractions containing larger amounts of peptides.

Samples were analyzed by means of reversed-phase nanoflow (300 nl/min) HPLC with nano-electrospray ionization using a quadrupole time-of-flight mass spectrometer (QSTAR Pulsar I, Applied Biosystems) operated in positive ion mode. MS/MS spectra were acquired in a data-dependent manner over the course of three injections and analyses selecting the top two most intense eluting ions in the 400–1600 *m/z* range with a 2+ to 5+ charge state. Following selection for MS/MS analysis, precursor ions were excluded from selection for MS/MS analysis for 180 s. Following the first 2 h of LC-MS/MS analysis, gas phase fractionation was used to increase the total number of identified peptides.

All MS/MS data were analyzed using Protein Pilot 2.0 (Applied Biosystems) (22). Raw data files were searched against the *Leishma-*

nia infantum proteome in TriTrypDB version 3.3. Peptides with confidence > 95% were considered for further analysis. Acceptable mass tolerances were 0.6 Da for MS and 0.25 Da for MS/MS. Protein Pilot has these as well as a list of considered post-translational modifications preconfigured in the search settings; therefore, high-confidence results meet these criteria.

All of the procedures described above were performed on two independent biological repeats.

Data Processing for the Time Course Experiment—The ratio of the peptide concentration at each time point (relative to promastigotes-0h) was calculated as either the average value of the two independent biological repeats or the single value if the peptide was detected in only one experiment. The values presented in the supplemental tables are $\log_2$-transformed. The data for the signal-specific phosphoproteomic experiment were processed in the same way. Statistical calculations were performed in R.

Cluster Analysis—Log_2-transformed values for the 163 phosphopeptides detected in all seven time-course samples were imported into MeV (23) and clustered with the Hierarchical Clustering - Support Trees (ST) module by constructing a gene tree with an optimized gene leaf order using Pearson correlation with absolute distance, complete linkage clustering, and 1000 bootstrap experiments. The tree was subsequently cut into eight clusters using a distance threshold of 1.0383358. Clusters were numbered according to the MeV convention. Clusters 4 + 5 and 2 + 6 were manually combined, as described in the text and figure legend.

Function Enrichment Analysis—We manually classified the proteins in 17 functional classes, namely, cell cycle, chaperone, cytoskeleton, degradation, development, DNA/RNA binding, DNA/RNA processing, histone, hypothetical, metabolism, protein kinase, protein phosphatase, ribosomal, signaling, translation, transporter, and other. We did not use Gene Ontology, as the *Leishmania* proteome is poorly annotated and therefore in most cases the Gene Ontology annotation does not go beyond a basic description of the molecular function of the protein. For each time point, we sorted the proteins according to their phosphorylation values and performed a gene set enrichment analysis (24).

Initiation of Phosphorylation/Dephosphorylation—To identify the initiation point of phosphorylation (or dephosphorylation), we identified, for each phosphopeptide, the minimum (or maximum for dephosphorylation) and maximum (or minimum) abundance values. The corresponding time points define, respectively, the beginning and end points of the analysis (phosphopeptides that had an absolute value of the maximum (minimum) < 0.5 were discarded). For each time point *j* in between, we then calculated two linear regression lines, one from promastigote to *j* and the other from *j* to amastigotes. The time point *j* for which the difference between the arctangent of the two regression lines was maximum (minimum) was then defined as the initiation point of phosphorylation (dephosphorylation) if both regression lines had an $R^2 \geq 0.7$.

RESULTS

Differentiation Induces Dynamic Changes in Protein Phosphorylation—In order to understand the kinetics of stage-specific protein phosphorylation during *L. donovani* promastigote-to-amastigote differentiation (18), we subjected titanium-dioxide-enriched phosphopeptides obtained at 0 (promastigotes), 2.5, 5 (phase I), 10 (phase II), 15 (phase III), 24, and 120 h (mature amastigotes, phase IV) after exposure to differentiation signal (8) to iTRAQ labeling followed by LC-MS/MS analysis. This analysis identified 708 phosphorylated sites in 572 peptides (corresponding to 282 distinct proteins), and the $\log_2$-transformed phosphopeptide abundance relative to promastigotes is listed in supplemental Table S1. Of the 572 peptides, 163 (containing 204 phosphorylation sites on 106 different proteins) were detected at all seven time points.

Hierarchical clustering of the relative abundance of these 163 phosphopeptides at all seven time points revealed six distinct kinetic profiles, as illustrated by the heat map and graphs in Figs. 1*A* and 1*B*, respectively. The largest group was cluster 8, which contained 58 phosphopeptides (from 47 proteins) that generally showed a ~2- to 8-fold increase in abundance beginning 2.5 to 10 h after signal exposure (phases I and II) and continued to increase in abundance at 15 h (phase III) before finally reaching ~4- to 16-fold at 120 h (mature amastigotes). Cluster 7 contained 28 phosphopeptides (from 23 proteins) that increased in abundance only late (in phase III or phase IV) to reach 1.5- to 4-fold greater values in amastigotes. Another group, comprising clusters 4 and 5, contained 28 phosphopeptides (from 26 proteins) that generally showed a transient increase of ~1.5- to 4-fold in phase I and/or II before returning to (or settling slightly above) promastigote levels at the onset of amastigote maturation (after 24 h). Cluster 3 contained 25 phosphopeptides (from 19 proteins) that remained largely unchanged until 10 h (phase II), when they began to decrease before finally reaching 2- to 4-fold lesser abundance in amastigotes. Another group, comprising clusters 2 and 6, contained 22 phosphopeptides (from 16 proteins) that generally decreased only late (phase IV) during differentiation to finally reach 1.5- to 4-fold reduced levels in amastigotes. Finally, cluster 1 contained three phosphopeptides (from three proteins) that showed transient down-regulation during differentiation, decreasing ~2-fold during phases I–III before increasing in phase IV. Not all phosphopeptides followed the consensus pattern described for each group, but the majority (131/163) showed at least a 2-fold change in abundance during the differentiation process. In addition, we detected another 225 phosphopeptides with >2-fold change in abundance during differentiation, but for which we lacked iTRAQ data from all seven time points.

Some of the most interesting patterns described in Fig. 1 are transient changes in phosphopeptide abundance (mostly in clusters 4 + 5 and 1, but also in some of the others), as these proteins are likely to be active (or inactive) only during the differentiation process. Fig. 2*A* illustrates 16 phosphopeptides that were transiently up-regulated by >2-fold during differentiation. Most of the peptides showed increased phosphorylation, beginning in phase I or II, which returned to promastigote levels during phase IV. The major exception was phosphorylation of S_{344} of LinJ.35.4450 (a conserved hypothetical protein), which showed an increase only at phase III. The abundance of the pS_{221}-containing phosphopeptide from LinJ.15.0370 (a putative ecotin) transiently increased by ~6-fold in phases I and II but subsequently decreased to only ~2-fold of promastigote levels in phase III and mature amas-

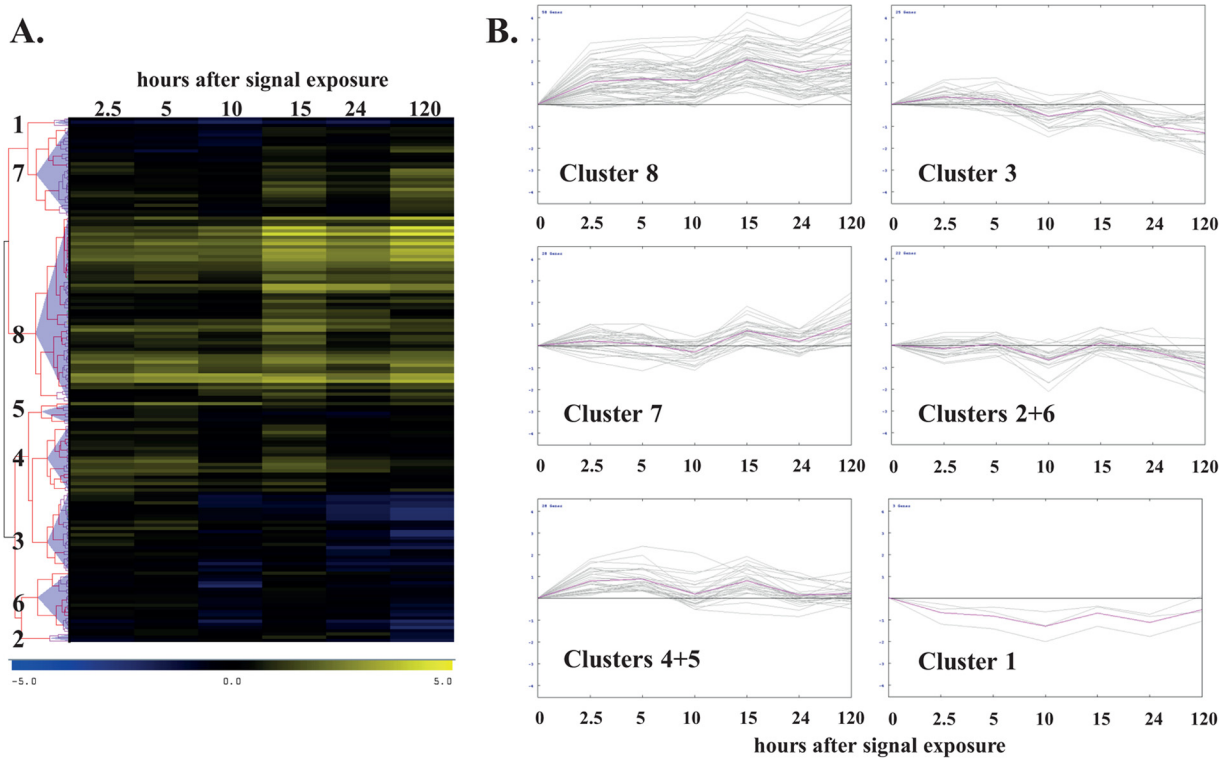


FIG. 1. ***A*, heatmap showing the HCL-ST clustering of Log_2 fold changes in phosphopeptide abundance during the differentiation time-course.** Cluster numbers assigned by MeV are shown to the left. *B*, graphical representation of abundance changes for peptides assigned to each cluster, with the mean values for each cluster represented as a pink line.

tigotes (Fig. 2*A*). Thus, it is likely that this protein is not phosphorylated in promastigotes and the differentiation signal specifically triggers phosphorylation of S_{221}. Our analysis also detected a transient increase in two phosphopeptides from LinJ.27.1300 (60S acidic ribosomal protein P0), with phosphorylation of S_{288} and S_{302} increasing ~2-fold during phase I and then gradually decreasing during phases II–IV, until the levels in mature amastigotes were ~3- to 5-fold lower than those in promastigotes (Fig. 2*A*). A phosphopeptide containing pS_{157} from LinJ.1040 (ribosomal protein S10) showed a similar (but only ~1.5-fold) transient increase in phosphorylation during phases I and II before the decreasing to ~2-fold below promastigote levels (see supplemental Table S1). These changes are in agreement with the previous observation (10) that protein synthesis is transiently up-regulated early in promastigote-to-amastigote differentiation, but the translation machinery is ultimately down-regulated in amastigotes.

Our analysis also indicated that the abundance of the phosphopeptide from LinJ.05.0140 (a putative nucleolar RNA helicase) containing pS_{24} transiently increased by ~2-fold in phase I before gradually returning to promastigote levels in mature amastigotes (Fig. 2*A*). In addition, we observed a transient (~2.6-fold) increase in phosphorylation of T_{216} of LinJ.33.0360 (HSP83–1) during phases I and II, before phosphorylation returned to promastigote levels in phase IV. The remaining proteins demonstrating transient up-regulation of phosphorylation have unknown functions, suggesting that a number of *Leishmania*- or trypansomatid-specific proteins play important roles in differentiation.

Four phosphopeptides showed a transient decrease in abundance of >2-fold during differentiation. The most interesting was the phosphopeptide containing $pS_{342}+pT_{346}$ from LinJ.34.2680 (regulatory subunit of protein kinase a-like protein), which showed a 4-fold decrease by 10 h before increasing to ~2-fold below promastigote levels in mature amastigotes (Fig. 2*B*). Three phosphopeptides from LinJ.36.6110 (hypothetical protein, conserved) all showed a similar (but less dramatic) pattern of transient decrease in first two phases before increasing in latter phases (Fig. 2*B* and supplemental Table S1). Two other conserved hypothetical proteins (LinJ.19.1150 and LinJ.33.1090) also showed transient dephosphorylation in phases I and II (Fig. 2*B*). Interestingly, the abundance of the phosphopeptides from both proteins recovered in phases III and IV, increasing to levels 1.5- to 2.8-fold higher than observed in promastigotes.

Different Phosphorylation Patterns on Proteins with Multiple Sites—In a previous study of the *Leishmania* phosphoproteome (18), we observed that many proteins contain more than one phosphorylation site, and that these sites can be distinctly and differentially phosphorylated between life stages. Therefore, here we compared the dynamics of abundance changes for different phosphopeptides from the same

ASBMB MOLECULAR & CELLULAR PROTEOMICS MCP

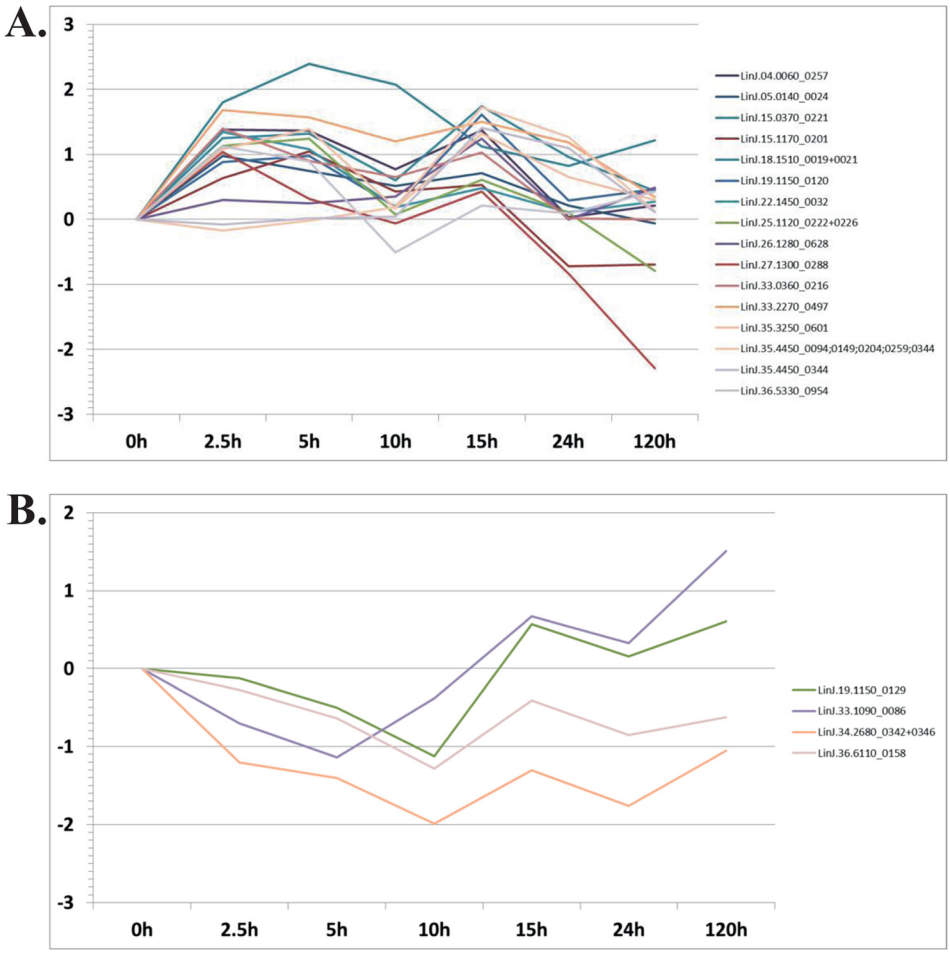


FIG. 2. ***A*, Log$_2$ fold abundance changes for phosphopeptides that display transient phosphorylation during differentiation.** The numbers after the "_" indicate the residue number of the phosphorylation site(s) in the respective protein. *B*, phosphopeptides that display transient dephosphorylation.

protein during promastigote-to-amastigote differentiation. Of the 106 proteins for which we had data from all seven time points, 33 were represented by at least two distinct phosphopeptides, and in most cases these demonstrated different kinetics for abundance changes. Of the 24 proteins with two distinct phosphorylation sites, 13 had phosphopeptides in different clusters (Fig. 3), meaning that their phosphorylation kinetics were different. Similarly, of five proteins with three sites, in only one case (LinJ.27.1300) were all three phosphopeptides found in the same cluster, and none of the proteins with more than three sites contained all the phosphopeptides in the same cluster (Fig. 3). These kinetic trends likely indicate phosphorylation of different regulatory domains by distinct protein kinases. As an example, the N terminus of the putative nucleolar RNA helicase (LinJ.05.0140) contains two distinct phosphorylation sites (S_{23} and S_{24}). As indicated above (Fig. 2*A*), the pS_{24}-containing phosphopeptide was in cluster 4 (Fig. 1), transiently increasing in abundance by ~2-fold in phase I, before gradually returning to promastigote levels in mature amastigotes. However, the phosphopeptide containing both pS_{23} andpS_{24} was in cluster 2 and decreased ~2-fold in phase IV (see supplemental Table S1). These results were confirmed (at early time points) by multiple reaction

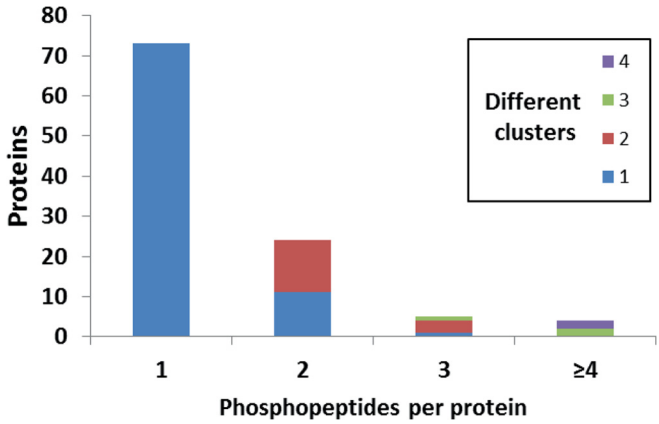


FIG. 3. **The number of phosphopeptides per protein in the time-course experiment.** Different colors indicate whether different phosphopeptides from the same protein show the same (blue) or different (red, green, or purple) kinetics.

TABLE I
Classes of proteins that were enriched for phosphorylation changes at different time points

Trend of phosphorylation	Time point					
	2.5 h	5 h	10 h	15 h	24 h	Amastigotes (120 h)
Up	Protein kinase		Metabolism	Translation	Chaperone	Chaperone Metabolism Protein kinase
Down		Ribosomal	Ribosomal transporter		Ribosomal transporter	Ribosomal transporter
	Phase I		Phase II	Phase III		Phase IV

"Up" denotes an increase in phosphorylation, and "down" denotes an increase in dephosphorylation.

monitoring (see supplemental Fig. S1*A*). Interestingly, multiple sequence alignment of LinJ.05.0140 orthologs revealed that the N-terminal 30 amino acids containing these phosphorylation sites are absent in other organisms (including *Trypanosoma* species) (supplemental Fig. S1*B*), suggesting a *Leishmania*-specific function for phosphorylation. We also observed a transient (~2.6-fold) increase in phosphorylation of T_{216} of HSP83–1 (LinJ.33.0360) during phases I and II (cluster 4) before phosphorylation returned to promastigote levels in phase IV (see Fig. 2*A*), whereas increased phosphorylation of S_{526} reached a peak of ~5-fold in phase III and remained elevated throughout differentiation into amastigotes (cluster 8 and supplemental Table S1).

Functional Classification of Phosphoproteins—Analysis of the phosphopeptides showing abundance changes during promastigote-to-amastigote differentiation revealed several classes of proteins that were enriched for phosphorylation changes (either up or down) at different time points (Table I). For instance, ribosomal components and transporters were enriched for dephosphorylation at 5, 10, 24, and 120 h, and translation machinery (other than ribosomal components) was enriched for phosphorylation at 15 h. Metabolic enzymes showed enrichment for increased abundance of phosphorylation at 10 and 120 h, chaperones were enriched at 24 and 120 h, and protein kinases were enriched at 2.5 and 120 h. These observations correlate well with our previous analysis of changes in protein and mRNA abundance (10, 11), suggesting that some changes in phosphopeptide abundance might be due to changes in protein abundance. Nevertheless, whether the changes in phosphopeptide abundance that we measured were due to differences in overall protein abundance or changes in the phosphorylation state of the protein, both serve to change the amount of phosphorylated protein present in the cell.

Signal-specific Phosphorylation in Phase I—In general, an increase in phosphopeptide abundance is more common than a decrease during promastigote-to-amastigote differentiation, primarily initiated in phases I and III (see Fig. 4 and supplemental Fig. S2). This is not unexpected, as signal perception occurs during phase I and morphological transition during phase III. In contrast, phases II and IV (which involve movement cessation and amastigote maturation, respectively) are almost exclusively associated with dephosphorylation events (Fig. 4 and supplemental Fig. S2). These observations prompted us to further analyze phosphorylation events associated with the two differentiation signals (temperature and pH) at the earliest time point, as this was the closest to signal perception and therefore might identify the proteins initiating the signaling pathway(s). Promastigotes were exposed to 37 °C and pH 7 (increased temperature only), 26 °C and pH 5.5 (lower pH only), and pH 5.5 and 37 °C (complete signal), and changes in phosphopeptide abundance were examined after 2.5 h using the same methodology as for the time-course experiment described above. A total of 355 phosphopeptides were detected in at least one sample (supplemental Table S2), with 319 quantified in all three samples. The $\log_2$ fold changes in abundance observed for each of these phosphopeptides are plotted in Fig. 5, and their variation among the three experimental conditions was assigned to one of the 27 possible patterns shown in Table II*A*. These patterns fell into three separate groups: 85 that failed to show >1.3-fold change under any condition, 77 that responded only to a partial signal (temperature or pH only), and 155 that responded to the full signal (increased temperature and lower pH (Table II*B*). As expected, the vast majority (143/155) of those that responded to the full signal showed an increase in abundance. In contrast, one-third of the 103 phosphopeptides responding to increased temperature only de-

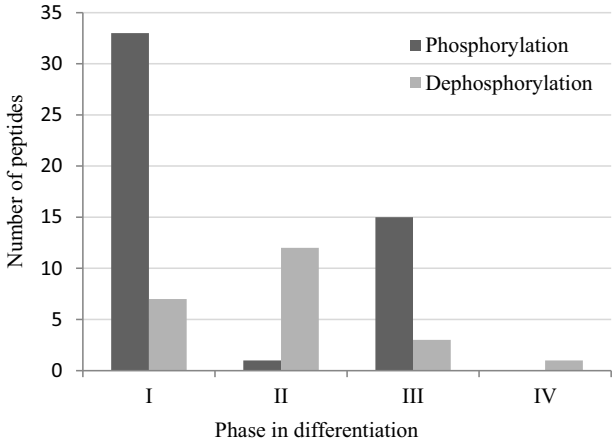


FIG. 4. **Initiation of peptide phosphorylation and dephosphorylation events at different phases of differentiation.**

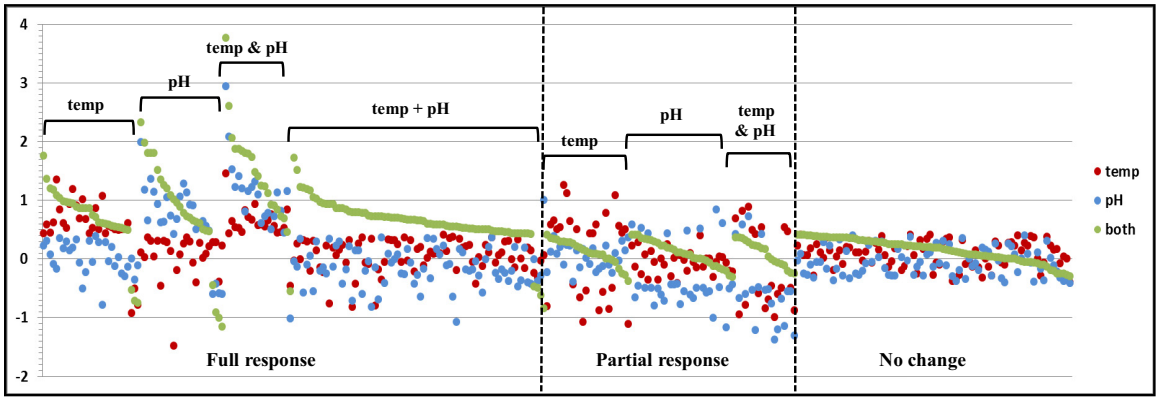


FIG. 5. **Log_2 fold-change values for the 319 phosphopeptides that were detected in all three conditions of the signal-dependent phosphorylation experiment (supplemental Table S2).** The values for each phosphopeptide after 2.5 h of exposure to 37 °C (red), pH (blue), and both (green) are represented by different positions along the *x*-axis of the graph. "Full response" indicates a change when exposed to both signals; "partial response" indicates a change when exposed to the temperature or pH signal alone. Changes that occurred in response to only temperature or pH are indicated at the top by "temp" or "pH," "temp & pH" indicates a change in response to both temperature and pH separately, and "temp+pH" indicates a change in response to only the complete signal (both temperature and pH together).

creased in abundance, and about half of the 115 that responded to lower pH only also decreased in abundance.

Remarkably, 78 phosphopeptides responded significantly only in the presence of both signals (of which 74 increased in abundance; Fig. 5). The eight proteins demonstrating >2-fold change in phosphorylation are shown in Fig. 6*A*. Strikingly, of the eight proteins, one, the putative serine/threonine protein kinase (LinJ.30.3640), increased by more than 3-fold only when exposed to the complete differentiation signal and was completely unaffected by acidic pH or elevated temperature alone. This finding further emphasizes the hypothesis that protein-kinase-mediated signaling pathways initiate differentiation. Two additional proteins that were affected only by the complete signal are involved in translation: LinJ.03.0960 (elongation initiation factor 2 α subunit) and LinJ.27.1300 (60S acidic ribosomal subunit protein P0).

Of the remaining phosphopeptides that changed in abundance after exposure to the full signal, 30 responded solely (or more robustly) to temperature, and 26 mostly to pH; 21 responded to both (Fig. 5; those with >2-fold change are shown in Figs. 6*B*, 6*C*, and 6*D*). The first group included HSP70 (LinJ.28.2960) and a threonyl-tRNA synthetase (LinJ.35.1420); the second group included ecotin (LinJ.15.0370), an ATP-dependent RNA helicase (LinJ.30.0930), serine palmitoyltransferase (LinJ.35.0320), an amastin-like protein (LinJ.30.0930), the regulatory subunit of a protein kinase A-like protein (LinJ.34.2680), a nucleobase transporter (LinJ.11.0520), and an RNA-binding protein (LinJ.35.2240). The last two were among the few showing dephosphorylation under these conditions. Another serine/threonine-protein kinase (LinJ.25.2450) contained two sites (S_{212} and T_{381}) that were phosphorylated by either temperature or pH alone, with an even greater (6- to 13-fold) increase upon exposure to the complete signal (Fig. 6*D*).

Possible Signaling Pathways Involved in Promastigote-to-amastigote Differentiation—The analyses described above identified 12 protein kinases, two protein kinase regulatory subunits, and four protein phosphatases (supplemental Table S1). For nine of these proteins, we have complete (or nearly complete) datasets for at least one phosphorylation site, allowing detailed analysis of the kinetics in response to the temperature and pH signals and during differentiation. Three protein kinases (LinJ.05.0390, LinJ.25.2450, and LinJ.35.1070) and one phosphatase (LinJ.36.2170) were phosphorylated during phase I (largely in response to both temperature and pH signals) and remained phosphorylated in amastigotes (Fig. 7*A*). Another kinase (LinJ.12.0016) and phosphatase (LinJ.22.1450) were transiently phosphorylated in phase I (in response to temperature + pH signals) but returned to (or fell below) promastigote levels during phases II and III, as well as in amastigotes (Fig. 7*B*).

Many of these signaling-related proteins contain multiple phosphorylation sites. For example, LinJ.35.1070 (a putative protein kinase) contains three sites (pS_{13}, pS_{378}, and pS_{408}). Both pS_{13} and pS_{378} showed a ~4-fold increase in phosphorylation at 2.5 h that gradually increased to 8-fold in amastigotes (Fig. 7*A*). Phosphorylation at pS_{408} appeared to increase slightly at 10 h, which is the only time point available. Similarly, all three phosphorylation sites of LinJ.12.0016 (a putative protein kinase) behaved with similar kinetics (although data were limited for S_{17} and are not shown in Fig. 7*B*). Interestingly, all three sites were very closely clustered (on the same tryptic fragment), but each peptide contained only a single phosphorylated residue, suggesting that this region might be the substrate of several different kinases.

LinJ.34.2680 (a putative regulatory subunit of kinase A found only in *Leishmania* and *T. cruzi* genomes) has at least 14

TABLE II

Summary of log_2 fold-change values for the 317 phosphopeptides that were detected in all three conditions of the signal-dependent phosphorylation experiment (supplemental Table S2 and Fig. 5)

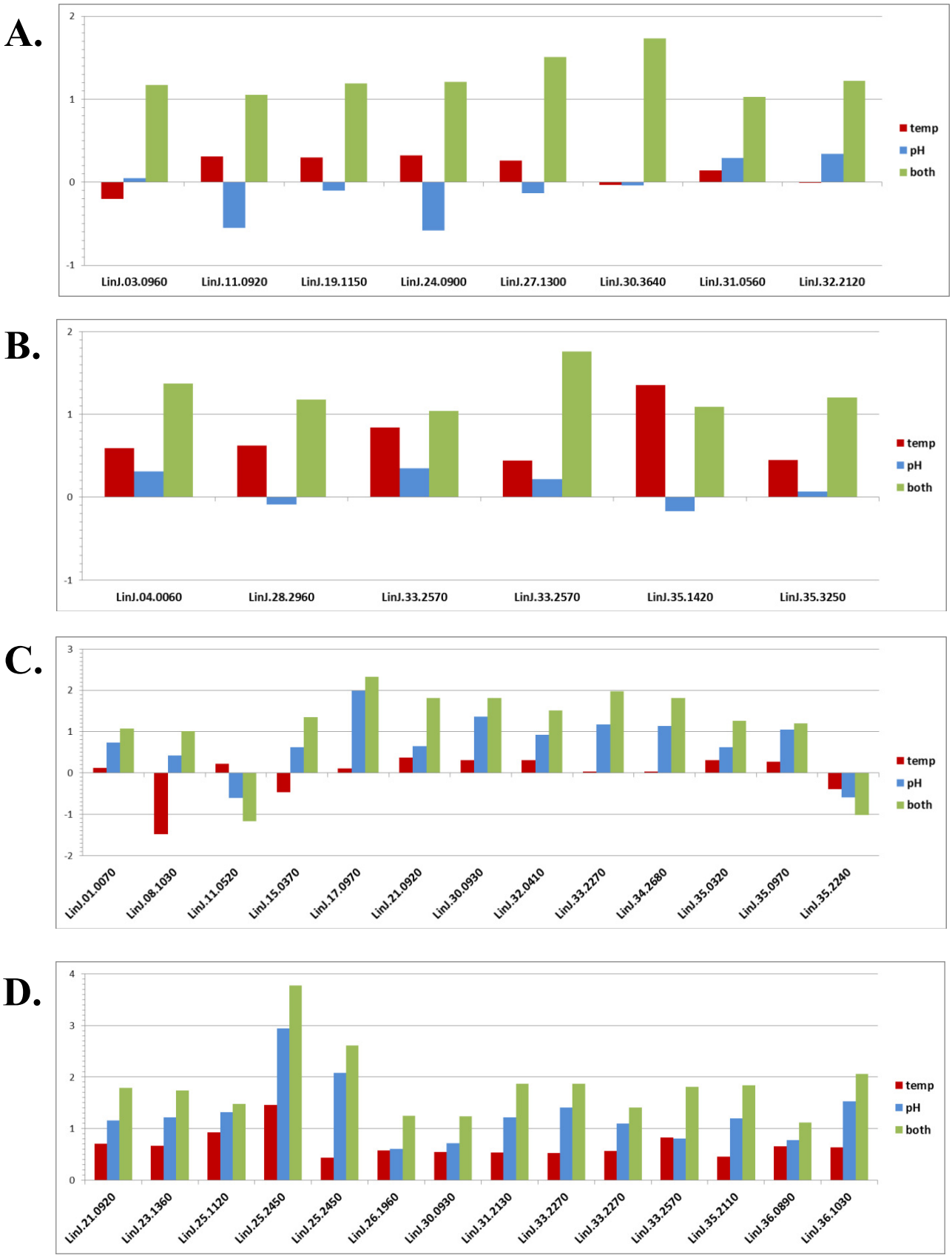
A, abundance changes were coded as "up" or "down" if they changed by more than 1.34-fold ($log_2 \geq 0.42$), and each phosphopeptide was manually assigned to 1 of 27 possible patterns.

Pattern	Code	Temperature	pH	pH + temperature	Count
1	UUU	Up	Up	Up	20
2	NUU	–	Up	Up	20
3	DUU	Down	Up	Up	2
4	UNU	Up	–	Up	25
5	NNU	–	–	Up	56
6	DNU	Down	–	Up	4
7	UDU	Up	Down	Up	2
8	NDU	–	Down	Up	13
9	DDU	Down	Down	Up	1
10	UUN	Up	Up	–	4
11	NUN	–	Up	–	8
12	DUN	Down	Up	–	0
13	UNN	Up	–	–	16
14	NNN	–	–	–	85
15	DNN	Down	–	–	10
16	UDN	Up	Down	–	4
17	NDN	–	Down	–	24
18	DDN	Down	Down	–	11
19	UUD	Up	Up	Down	0
20	NUD	–	Up	Down	1
21	DUD	Down	Up	Down	0
22	UND	Up	–	Down	0
23	NND	–	–	Down	3
24	DND	Down	–	Down	3
25	UDD	Up	Down	Down	0
26	NDD	–	Down	Down	4
27	DDD	Down	Down	Down	1
Up		71	55	143	
No change		214	202	162	
Down		32	60	12	

B, these patterns were used to ascribe a signal-dependent response to each phosphopeptide.

Response	Signal	Pattern(s)	Number of peptides	
Full	Temperature alone	4 + 7 + 21 + 24	30	155
	pH only	2 + 3 + 25 + 26	26	
	Temperature and pH	1 + 27	21	
	Temperature + pH	5 + 6 + 8 + 9 + 19 + 20 + 22 + 23	78	
Partial	Temperature only	13 + 15	26	77
	pH only	11 + 17	32	
	Temperature and pH only	10 + 12 + 16 + 18	19	
No change	None	14	85	85

different phosphorylation sites that demonstrate a considerably more complex phosphorylation profile (Fig. 7*C*). T_{262} showed a 4- to 6-fold increase in phosphorylation during phase I and remained at this level thereafter, whereas pS_{342} and pT_{346} were both dephosphorylated (together) by 2- to 4-fold with similar kinetics. In contrast, phosphorylation of S_{246} increased by ~2- to 3-fold in phases III and IV. Although there are more limited data for the other sites, some hints of their patterns can be gleaned from the time points at which they were measured. S_{121} and S_{123} appeared to be phosphorylated (separately) in a manner similar to T_{262}. Phosphorylation of S_{247} was similar to that of S_{246}, although the $pS_{246}+pS_{247}$ double phosphopeptide showed no significant change in abundance. Phosphorylation of S_{332} was also upregulated in phases III and IV in a manner similar to that of S_{246}. However, S_{124} was dephosphorylated (at least in stages III and IV) with kinetics similar to those of $pS_{342}+pT_{346}$, whereas the $pS_{329}+pS_{332}$ phosphopeptide decreased in abundance in parallel with $pS_{342}+pT_{346}$ in phase I. Interestingly, all of these changes in phosphorylation appeared to be in response to the pH signal, although phosphorylation of T_{262} may be synergized by elevated temperature.


A.
2
1
0
-1
temp
pH
both
LinJ.03.0960
LinJ.11.0920
LinJ.19.1150
LinJ.24.0900
LinJ.27.1300
LinJ.30.3640
LinJ.31.0560
LinJ.32.2120
B.
2
1
0
-1
temp
pH
both
LinJ.04.0060
LinJ.28.2960
LinJ.33.2570
LinJ.33.2570
LinJ.35.1420
LinJ.35.3250
C.
3
2
1
0
-1
-2
temp
pH
both
LinJ.01.0070
LinJ.08.1030
LinJ.11.0520
LinJ.15.0370
LinJ.17.0970
LinJ.21.0920
LinJ.30.0930
LinJ.32.0410
LinJ.33.2270
LinJ.34.2680
LinJ.35.0320
LinJ.35.0970
LinJ.35.2240
D.
4
3
2
1
0
temp
pH
both
LinJ.21.0920
LinJ.23.1360
LinJ.25.1120
LinJ.25.2450
LinJ.25.2450
LinJ.26.1960
LinJ.30.0930
LinJ.31.2130
LinJ.33.2270
LinJ.33.2270
LinJ.33.2570
LinJ.35.2110
LinJ.36.0890
LinJ.36.1030

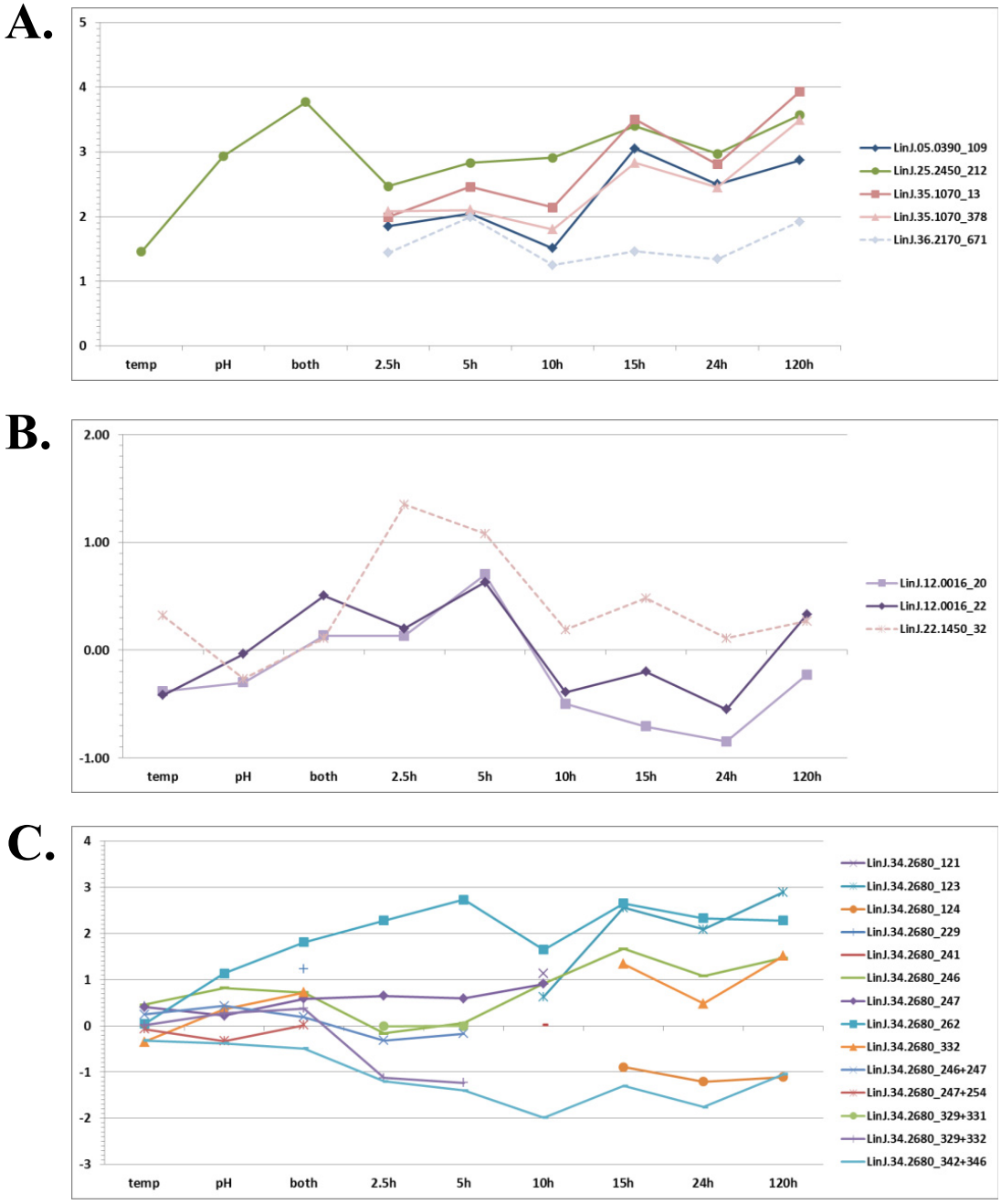


FIG. 7. ***A*, protein kinases and phosphatase that were phosphorylated during phase I and remained phosphorylated throughout differentiation.** *B*, protein kinases and a phosphatase that were transiently phosphorylated. *C*, phosphorylation kinetics of different sites in the multiply phosphorylated protein kinase A regulatory subunit like-protein (PKAR'). Values are presented as Log_2 fold change from promastigotes.

Although the functional significance of these complex and many-fold changes in protein phosphorylation during promastigote-to-amastigote differentiation is not yet fully understood, the substantial number of proteins involved and the variety of their patterns of changes underscore their likely importance.

FIG. 6. ***A*, phosphopeptides that showed >2-fold change in phosphorylation only in response to the full signal.** *B*, phosphopeptides that showed >2-fold change in phosphorylation in response to the full signal and were also affected by temperature. *C*, phosphopeptides that showed >2-fold change in phosphorylation in response to the full signal and were also affected by pH. *D*, phosphopeptides that showed >2-fold change in phosphorylation in response to the full signal and were also affected by temperature and pH separately. Values are presented as Log_2 fold change from promastigotes.

ASBMB MOLECULAR & CELLULAR PROTEOMICS MCP

ASBMB MOLECULAR & CELLULAR PROTEOMICS MCP

DISCUSSION

The host-free system we developed to simulate *Leishmania* differentiation inside its host has, to date, provided significant insight into the mechanisms of this process. Comparative analysis of genome-wide time-course transcriptomic and proteomic datasets clearly indicated that promastigote-to-amastigote differentiation is a regulated and highly coordinated process. Here, we have provided an additional layer to these analyses by employing iTRAQ affinity tagging to quantitatively analyze changes in phosphopeptide abundance and describing the dynamics of protein phosphorylation during *L. donovani* differentiation. In a recent study, using shotgun phosphoproteomics, we demonstrated that in axenic *L. donovani* there is more stage-specific (*i.e.* in promastigotes or amastigotes exclusively) than constitutive (*i.e.* in both life stages) protein phosphorylation (18). In this work, we determined the kinetics of changes that lead to these stage-specific phosphorylation events.

The results revealed that even some proteins that were equally phosphorylated in promastigotes and amastigotes underwent a transient change in phosphorylation abundance during differentiation (*i.e.* phosphorylation abundance was up- or down-regulated during one or two phases of differentiation). These transient changes in protein phosphorylation add to similar changes in mRNA and protein abundance observed during differentiation (9–11). The phenomenon of transient change that occurs at all levels of gene expression is indicative of its significance in *Leishmania* development inside the host. The factors that regulate these processes are yet unknown, but because *Leishmania* lack transcriptional regulation of protein-coding genes, we hypothesize that novel mechanisms that control mRNA maturation contribute to these transient changes, together with elements that influence translation and post-translational processes. Preliminary analysis carried out in our laboratory indicated that transient changes in spliced leader RNA abundance during the first two phases of *L. donovani* differentiation correlate with some of the variations in mRNA abundance.[2]

To date, there is no model available for the dynamics of phosphorylation-mediated developmental processes in single-cell eukaryotes, including parasitic protozoa. Two studies have analyzed phosphoproteomes of lower multicellular organisms, nematode larva (25) and barnacle (26); both used two-dimensional gel electrophoresis and found interesting stage-specific, as well as constitutive, protein phosphorylation. Similar analyses have been carried out in mammals, with protein phosphorylation dynamics being analyzed during early stages of embryonic stem cell development (27) and in brain nuclear proteins (28). Other studies in mammalian cells monitored time-dependent changes in protein phosphorylation abundance in response to epidermal growth factor stimulation (29, 30), observing that for multiply phosphorylated proteins, different sites showed different dynamics trends. As we found similar results during *L. donovani* differentiation, the existence of proteins that possess many sites with different trends appears global, as it exists from lower to most developed eukaryotes. It also indicates that although different kinases are responsible for the phosphorylation of the different sites, they must be coordinated in order to properly regulate protein function.

An extreme example of a multiply phosphorylated protein identified in the current work is the *Leishmania* homolog of the regulatory subunit of protein kinase A (LdPKAR', LinJ.34.2680). In mammalian cells, cAMP-dependent PKA has four regulatory subunit isoforms that negatively regulate activity of its catalytic kinase subunit (31). In African trypanosomes, extracellular parasites that cause African sleeping sickness, PKA activity is independent of cAMP,[3] and their genomes contain only a single regulatory subunit gene (TbPKAR1, Tb11.02.2210). In contrast, the genomes of the intracellular trypanosomatids *T. cruzi* and *Leishmania* contain genes that encode for two different regulatory subunit homologs, Linj.13.0160 and Linj.34.2680, of which the former is likely the ortholog of TbPKAR1. Proteins derived from these genes are 30% and 35% identical, respectively, to the corresponding cAMP-dependent PKA-R1 protein in humans. The current study indicates there are at least three different dynamic trends of the phosphorylation in LdPKAR', whereas we observed no phosphorylation of PKAR1. These changes suggest that LdPKAR' likely has a role in differentiation; however, whether it regulates this process via interaction with one (or more) of the catalytic subunits of PKA is still to be investigated. Interestingly, one of the catalytic subunits (LdPKAC3, LinJ.18.1090) was phosphorylated only in response to the complete differentiation signal (see supplemental Table S2).

Most interesting are phosphorylation events that occur early in differentiation, especially in protein kinases. These are likely part of the differentiation initiation pathway. Our analysis detected three additional protein kinases (LinJ.05.0390, LinJ.25.2450, and LinJ.35.1070) whose phosphorylation increased markedly in phase I, suggesting they either underwent autophosphorylation in response to a differentiation signal or were phosphorylated by protein kinases further upstream in the differentiation activation pathway.

Also of interest are enzymes that are significantly phosphorylated early in phase I (2.5 h after signal exposure). Most significant were asparagine synthetase (LinJ.26.0790) and heat shock protein DNAJ (LinJ.27.2350). Asparagine synthetase underwent an almost 5-fold increase in phosphorylation of S_{226}, and levels remained high throughout differentiation (8-fold in amastigotes). In contrast, the protein abundance of asparagine synthetase started to decrease at 15 h, reaching

[2] Lahav *et al.*, in preparation.

[3] Dr. Michael Boshart, personal communication.

half the promastigote level in amastigotes (11). Heat shock protein DNAJ is phosphorylated on S_{89}, and phosphorylation of this residue increased by 3.5-fold at 2.5 h, reaching >22-fold in amastigotes. Such a dramatic increase in phosphorylation abundance indicates that the protein is likely not phosphorylated in promastigotes and that its phosphorylation is initiated after the parasites start to differentiate. In contrast, the abundance of this protein remained unchanged throughout differentiation, showing only a mild decrease in amastigotes (11). Thus, for both proteins, a net change in protein phosphorylation was observed, suggesting that these changes affect protein function.

An interesting observation was the relationship between phosphorylation activity and differentiation phase. Phases I and III were enriched with protein phosphorylation activity, whereas dephosphorylation activity was more abundant in phases II and IV. These changes correlated with the activity that is typical of each phase. For example, signal perception prepares promastigotes to start differentiating. Cells cease movement and aggregate in phase II. A process of preparation is likely to require a significant amount of change in protein activity, some of which is mediated by phosphorylation and other post-translational modifications.

Importantly, we detected signal-specific phosphorylation for a large number of proteins, including a protein kinase (LinJ.30.3640). Phosphorylation of this protein increased by more than 3-fold only when promastigotes were exposed to the complete differentiation signal (pH 5.5 and 37 °C together), and not when the signal was deconvoluted (pH 5.5 or 37 °C separately). We hypothesize that this protein kinase has an essential role in the pathway that transduces the differentiation signal.

This work constitutes the first study of the time-course phosphoproteome dynamics of parasitic protozoa. Using a host-free system that simulates intracellular development allowed for major improvement in the attempt to identify the signaling pathway that initiates *Leishmania* differentiation.

The mass spectrometry proteomics data have been deposited to the ProteomeXchange Consortium (http://proteomecentral.proteomexchange.org) via the PRIDE partner repository (32) with the dataset identifier PXD000671.

Acknowledgments—We thank Professor Christoph Borchers and Dr. Derek Smith from the University of Victoria Proteomics Center, Canada, for the iTRAQ and MS assays.

* This work was supported by the seventh Framework Programme of the European Commission through a grant to the LEISHDRUG program, U.S.-Israel Binational Foundation grant 2009226 and by Grant Number 33928 from the Chief Scientist of the Israel Ministry of Health Foundation. The data deposition to the ProteomeXchange Consortium was supported by PRIDE Team, EBI.

S This article contains supplemental material.

§§ To whom correspondence should be addressed. Tel.: 972-4-2893647; Fax: 972-4-8225153; E-mail: danz@bi.technion.ac.il.

REFERENCES

1. Herwaldt, B. L. (1999) Leishmaniasis. *Lancet* **354,** 1191–1199
2. Murray, H. W., Berman, J. D., Davies, C. R., and Saravia, N. G. (2005) Advances in leishmaniasis. *Lancet* **366,** 1561–1577
3. McConville, M. J., and Naderer, T. (2011) Metabolic pathways required for the intracellular survival of *Leishmania. Annu. Rev. Microbiol.* **65,** 543–561
4. Zilberstein, D. (2008) Physiological and biochemical aspects of *Leishmania* development. In *Leishmania After the Genome: Biology and Control* (Myler, P. J., and Fasel, N., eds), pp. 107–122, Horizon Scientific Press and Caiser Academic Press, New York
5. Saar, Y., Ransford, A., Waldman, E., Mazareb, S., Amin-Spector, S., Plumblee, J., Turco, S. J., and Zilberstein, D. (1998) Characterization of developmentally-regulated activities in axenic amastigotes of *Leishmania* donovani. *Mol. Biochem. Parasitol.* **95,** 9–20
6. Debrabant, A., Joshi, M. B., Pimenta, P. F., and Dwyer, D. M. (2004) Generation of *Leishmania donovani* axenic amastigotes: their growth and biological characteristics. *Int. J. Parasitol.* **34,** 205–217
7. Bates, P. A., Robertson, C. D., Tetley, L., and Coombs, G. H. (1992) Axenic cultivation and characterization of *Leishmania* mexicana amastigote-like forms. *Parasitology* **105(Pt 2),** 193–202
8. Barak, E., Amin-Spector, S., Gerliak, E., Goyard, S., Holland, N., and Zilberstein, D. (2005) Differentiation of *Leishmania donovani* in host-free system: analysis of signal perception and response. *Mol. Biochem. Parasitol.* **141,** 99–108
9. Saxena, A., Lahav, T., Holland, N., Aggarwal, G., Anupama, A., Huang, Y., Volpin, H., Myler, P. J., and Zilberstein, D. (2007) Analysis of the *Leishmania donovani* transcriptome reveals an ordered progression of transient and permanent changes in gene expression during differentiation. *Mol. Biochem. Parasitol.* **152,** 53–65
10. Lahav, T., Sivam, D., Volpin, H., Ronen, M., Tsigankov, P., Green, A., Holland, N., Kuzyk, M., Borchers, C., Zilberstein, D., and Myler, P. J. (2011) Multiple levels of gene regulation mediate differentiation of the intracellular pathogen *Leishmania. FASEB J.* **25,** 515–525
11. Rosenzweig, D., Smith, D., Opperdoes, F., Stern, S., Olafson, R. W., and Zilberstein, D. (2008) Retooling *Leishmania* metabolism: from sand fly gut to human macrophage. *FASEB J.* **22,** 590–602
12. Cloutier, S., Laverdiere, M., Chou, M. N., Boilard, N., Chow, C., and Papadopoulou, B. (2012) Translational control through eIF2alpha phosphorylation during the *Leishmania* differentiation process. *PLoS ONE* **7,** e35085
13. Mottram, J. C., and Coombs, G. H. (1985) *Leishmania* mexicana: enzyme activities of amastigotes and promastigotes and their inhibition by antimonials and arsenicals. *Exp. Parasitol.* **59,** 151–160
14. Naderer, T., Ellis, M. A., Sernee, M. F., De Souza, D. P., Curtis, J., Handman, E., and McConville, M. J. (2006) Virulence of *Leishmania* major in macrophages and mice requires the gluconeogenic enzyme fructose-1,6-bisphosphatase. *Proc. Natl. Acad. Sci. U.S.A.* **103,** 5502–5507
15. Tsigankov, P., Gherardini, P. F., Helmer-Citterich, M., and Zilberstein, D. (2012) What has proteomics taught us about *Leishmania* development? *Parasitology* **139,** 1146–1157
16. Rosenzweig, D., Smith, D., Myler, P. J., Olafson, R. W., and Zilberstein, D. (2008) Post-translational modification of cellular proteins during *Leishmania donovani* differentiation. *Proteomics* **8,** 1843–1850
17. Ptacek, J., Devgan, G., Michaud, G., Zhu, H., Zhu, X., Fasolo, J., Guo, H., Jona, G., Breitkreutz, A., Sopko, R., McCartney, R. R., Schmidt, M. C., Rachidi, N., Lee, S. J., Mah, A. S., Meng, L., Stark, M. J., Stern, D. F., De Virgilio, C., Tyers, M., Andrews, B., Gerstein, M., Schweitzer, B., Predki, P. F., and Snyder, M. (2005) Global analysis of protein phosphorylation in yeast. *Nature* **438,** 679–684
18. Tsigankov, P., Gherardini, P. F., Helmer-Citterich, M., Spath, G. F., and Zilberstein, D. (2013) Phosphoproteomic analysis of differentiating *Leishmania* parasites reveals a unique stage-specific phosphorylation motif. *J. Proteome Res.* **12,** 3405–3412
19. Morales, M. A., Watanabe, R., Laurent, C., Lenormand, P., Rousselle, J. C., Namane, A., and Spath, G. F. (2008) Phosphoproteomic analysis of *Leishmania donovani* pro- and amastigote stages. *Proteomics* **8,** 350–363
20. Zimmermann, S., Moll, H., Solbach, W., and Luder, C. G. (2009) Meeting Report IFoLeish-2008: current status and future challenges in *Leishmania* research and leishmaniasis. *Protist* **160,** 151–158
21. Morales, M. A., Watanabe, R., Dacher, M., Chafey, P., Osorio y Fortea, J.,

ASBMB MOLECULAR & CELLULAR PROTEOMICS MCP

Scott, D. A., Beverley, S. M., Ommen, G., Clos, J., Hem, S., Lenormand, P., Rousselle, J. C., Namane, A., and Spath, G. F. (2010) Phosphoproteome dynamics reveal heat-shock protein complexes specific to the *Leishmania donovani* infectious stage. *Proc. Natl. Acad. Sci. U.S.A.* **107,** 8381–8386

22. Shilov, I. V., Seymour, S. L., Patel, A. A., Loboda, A., Tang, W. H., Keating, S. P., Hunter, C. L., Nuwaysir, L. M., and Schaeffer, D. A. (2007) The Paragon Algorithm, a next generation search engine that uses sequence temperature values and feature probabilities to identify peptides from tandem mass spectra. *Mol. Cell. Proteomics* **6,** 1638–1655
23. Saeed, A. I., Sharov, V., White, J., Li, J., Liang, W., Bhagabati, N., Braisted, J., Klapa, M., Currier, T., Thiagarajan, M., Sturn, A., Snuffin, M., Rezantsev, A., Popov, D., Ryltsov, A., Kostukovich, E., Borisovsky, I., Liu, Z., Vinsavich, A., Trush, V., and Quackenbush, J. (2003) TM4: a free, open-source system for microarray data management and analysis. *Biotechniques* **34,** 374–378
24. Subramanian, A., Tamayo, P., Mootha, V. K., Mukherjee, S., Ebert, B. L., Gillette, M. A., Paulovich, A., Pomeroy, S. L., Golub, T. R., Lander, E. S., and Mesirov, J. P. (2005) Gene set enrichment analysis: a knowledge-based approach for interpreting genome-wide expression profiles. *Proc. Natl. Acad. Sci. U.S.A.* **102,** 15545–15550
25. Chandramouli, K. H., Mok, F. S., Wang, H., and Qian, P. Y. (2011) Phosphoproteome analysis during larval development and metamorphosis in the spionid polychaete Pseudopolydora vexillosa. *BMC Dev. Biol.* **11,** 31
26. Zhang, Y., Xu, Y., Arellano, S. M., Xiao, K., and Qian, P. Y. (2010) Comparative proteome and phosphoproteome analyses during cyprid development of the barnacle Balanus (=Amphibalanus) amphitrite. *J. Proteome Res.* **9,** 3146–3157
27. Van Hoof, D., Munoz, J., Braam, S. R., Pinkse, M. W., Linding, R., Heck, A. J., Mummery, C. L., and Krijgsveld, J. (2009) Phosphorylation dynamics during early differentiation of human embryonic stem cells. *Cell Stem Cell* **5,** 214–226
28. Liao, L., McClatchy, D. B., Park, S. K., Xu, T., Lu, B., and Yates, J. R., 3rd (2008) Quantitative analysis of brain nuclear phosphoproteins identifies developmentally regulated phosphorylation events. *J. Proteome Res.* **7,** 4743–4755
29. Morandell, S., Stasyk, T., Skvortsov, S., Ascher, S., and Huber, L. A. (2008) Quantitative proteomics and phosphoproteomics reveal novel insights into complexity and dynamics of the EGFR signaling network. *Proteomics* **8,** 4383–4401
30. Olsen, J. V., Blagoev, B., Gnad, F., Macek, B., Kumar, C., Mortensen, P., and Mann, M. (2006) Global, in vivo, and site-specific phosphorylation dynamics in signaling networks. *Cell* **127,** 635–648
31. Skalhegg, B. S., and Tasken, K. (2000) Specificity in the cAMP/PKA signaling pathway. Differential expression, regulation, and subcellular localization of subunits of PKA. *Front. Biosci.* **5,** D678–D693
32. Vizcaino, J. A., Cote, R. G., Csordas, A., Dianes, J. A., Fabregat, A., Foster, J. M., Griss, J., Alpi, E., Birim, M., Contell, J., O'Kelly, G., Schoenegger, A., Ovelleiro, D., Perez-Riverol, Y., Reisinger, F., Rios, D., Wang, R., and Hermjakob, H. (2013) The PRoteomics IDEntifications (PRIDE) database and associated tools: status in 2013. *Nucleic Acids Res.* **41,** D1063–D1069

ASBMB MOLECULAR & CELLULAR PROTEOMICS MCP